ORIGINAL ARTICLE

Imaging the Respiratory Transition at Birth
Unraveling the Complexities of the First Breaths of Life

David G. Tingay[1,2,3,4], Olivia Farrell[1,2], Jessica Thomson[1,2], Elizabeth J. Perkins[1], Prue M. Pereira-Fantini[1,2], Andreas D. Waldmann[5], Christoph Rüegger[4], Andy Adler[6], Peter G. Davis[4], and Inéz Frerichs[7]

[1]Neonatal Research, Murdoch Children's Research Institute, Melbourne, Australia; [2]Department of Paediatrics, University of Melbourne, Melbourne, Australia; [3]Neonatology, Royal Children's Hospital, Melbourne, Australia; [4]Neonatal Research, The Royal Women's Hospital, Melbourne, Australia; [5]Department of Anesthesiology and Intensive Care Medicine, Rostock University Medical Center, Germany; [6]Department of Systems and Computer Engineering, Carleton University, Ottawa, Ontario, Canada; and [7]Department of Anaesthesiology and Intensive Care Medicine, University Medical Centre Schleswig-Holstein, Campus Kiel, Kiel, Germany

ORCID IDs: 0000-0003-1522-4691 (D.G.T.); 0000-0003-1496-2625 (C.R.); 0000-0002-2312-5346 (A.A.); 0000-0001-6742-7314 (P.G.D.); 0000-0002-7712-6539 (I.F.).

Abstract

Rationale: The transition to air breathing at birth is a seminal respiratory event common to all humans, but the intrathoracic processes remain poorly understood.

Objectives: The objectives of this prospective, observational study were to describe the spatiotemporal gas flow, aeration, and ventilation patterns within the lung in term neonates undergoing successful respiratory transition.

Methods: Electrical impedance tomography was used to image intrathoracic volume patterns for every breath until 6 minutes from birth in neonates born by elective cesearean section and not needing resuscitation. Breaths were classified by video data, and measures of lung aeration, tidal flow conditions, and intrathoracic volume distribution calculated for each inflation.

Measurements and Main Results: A total of 1,401 breaths from 17 neonates met all eligibility and data analysis criteria. Stable FRC was obtained by median (interquartile range) 43 (21–77) breaths. Breathing patterns changed from predominantly crying (80.9% first min) to tidal breathing (65.3% sixth min). From birth, tidal ventilation was not uniform within the lung, favoring the right and nondependent regions; $P < 0.001$ versus left and dependent regions (mixed-effects model). Initial crying created a unique volumetric pattern with delayed midexpiratory gas flow associated with intrathoracic volume redistribution (pendelluft flow) within the lung. This preserved FRC, especially within the dorsal and right regions.

Conclusions: The commencement of air breathing at birth generates unique flow and volume states associated with marked spatiotemporal ventilation inhomogeneity not seen elsewhere in respiratory physiology. At birth, neonates innately brake expiratory flow to defend FRC gains and redistribute gas to less aerated regions.

Keywords: neonate; electrical impedance tomography; birth; ventilation; aeration

(Received in original form July 29, 2020; accepted in final form December 20, 2020)

Supported by the Victorian Government Operational Infrastructure Support Program (Melbourne, Australia) and a grant from the National Health and Medical Research Council Centre of Research Excellence (grant 1057514). D.G.T. is supported by a National Health and Medical Research Council Clinical Career Development Fellowship (grant 1053889). P.G.D. is supported by a National Health and Medical Research Council Program grant (grant 606789) and by a National Health and Medical Research Council Practitioner Fellowship (grant 556600).

Author Contributions: D.G.T. developed the concept and designed the experiment. D.G.T., O.F., J.T., E.J.P., and C.R. enrolled and studied all infants. D.G.T., A.D.W., A.A., and I.F. developed the image reconstruction and analysis methods used in the study. D.G.T., O.F., J.T., and P.M.P.-F. were involved in data analysis. D.G.T., A.A., P.G.D., and I.F. interpreted the data. D.G.T. wrote the first draft of the manuscript and all authors contributed to redrafting the manuscript.

Correspondence and requests for reprints should be addressed to David G. Tingay, M.B. B.S., D.C.H., F. R.A.C.P., Ph.D., Neonatal Research, Murdoch Children's Research Institute, Royal Children's Hospital, Flemington Road, Parkville 3052, Victoria, Australia. E-mail: david.tingay@rch.org.au.

Data sharing statement: Individual participant data collected during the study, after deidentification, and study protocols and statistical analysis code are available beginning 3 months and ending 23 years after article publication to researchers who provide a methodological sound proposal with approval by an independent review committee ("learned intermediary") identified for purpose. Data are available for analysis to achieve aims in the approved proposal. Proposals should be directed to david.tingay@mcri.edu.au; to gain access, data requestors will need to sign a data access or material transfer agreement approved by the Murdoch Children's Research Institute.

This article has a related editorial.

This article has an online supplement, which is accessible from this issue's table of contents at www.atsjournals.org.

Am J Respir Crit Care Med Vol 204, Iss 1, pp 82–91, Jul 1, 2021

Originally Published in Press as DOI: 10.1164/rccm.202007-2997OC on February 5, 2021
Internet address: www.atsjournals.org

At a Glance Commentary

Scientific Knowledge on the Subject: Birth requires the rapid transition from a fluid-filled to aerated lung, a process that is poorly understood. Limited human and animal studies suggest high intrathoracic pressure and flow states are required to attain FRC and support tidal ventilation.

What This Study Adds to the Field: This is the first breath-by-breath imaging of the lungs of term neonates undergoing successful respiratory transition at birth. We identified highly inhomogeneous spatiotemporal aeration and ventilation patterns. Crying at birth preserved FRC by allowing intrathoracic volume redistribution (pendelluft flow) within the lung. Newborns defend aeration from intrathoracic lung fluid shifts at birth by innately braking expiratory flow using the glottis and diaphragm.

The rapid adaptation to air-breathing at birth (aeration) is one of the most important, but least understood, physiological events in humans. Much of our understanding is inferred from preclinical studies (1–4) or invasive observational studies (5–8). These studies suggest that creating an FRC during the initial process of lung aeration requires first clearing the airways of fetal lung liquid using high intrathoracic pressure gradients (1, 2, 5). Subsequent tidal ventilation must prevent an influx of fluid back into the alveoli during expiration (1). Animal studies have demonstrated that these processes exhibit a high degree of spatiotemporal variability within the lung (2, 9). For most newborns, fluid clearance and the transition from the placenta to the lungs as the organ of gas exchange is achieved through the spontaneous onset of breathing. When this process fails, especially in preterm infants, death or significant morbidity may result. Because of an inability to define the processes of aeration and ventilation at birth, effective evidence-based interventions to support breathing after birth are lacking (10, 11).

The development of effective delivery room interventions first requires an understanding of the physiological processes defining success or failure of aeration at birth. Adapting physiological concepts from preclinical studies have limited utility, as instrumentation restricts the ability to emulate respiratory mechanics and the neurological state of the breathing human infant (1–3, 12). The delivery room further creates a challenging research environment, the time-critical and dynamic nature of birth itself hampers physiological measurements (13). Lung volume changes at birth have been intermittently imaged using chest radiography (14) and ultrasound (15), and pressure and flow patterns have been measured invasively at the mouth or pharynx (5, 16). These studies identified unique breath types associated with high intrathoracic pressure gradients during successful respiratory transition in term infants, specifically, crying and grunting (5, 17, 18). Importantly, these studies failed to directly define the fundamental dynamic spatiotemporal processes of aeration and subsequent ventilation within the lung.

To address this gap in knowledge, we used electrical impedance tomography (EIT), an emerging radiation-free imaging modality (19). EIT uses the differential electrical properties of aerated and fluid-containing tissue to measure the tidal and end-expiratory volume changes in lung regions within a transverse chest slice (19). We adapted our EIT techniques for measuring the respiratory transition in preclinical studies (2–4, 12, 20–23). This allowed noninvasive and nonhazardous direct imaging of the dynamic breath-to-breath regional process of aeration at birth in human infants without interfering with normal physiology or clinical care. The objective of this study was to describe the spatiotemporal respiratory patterns associated with the successful transition to air-breathing after birth in term infants. The specific aims were to *1*) characterize the inspiratory and expiratory time and flow characteristics within the lung at birth and *2*) describe the resultant spatiotemporal ventilation and volume patterns by breath type and time.

Some of the results of these studies have been previously reported in the form of a preprint (medRxiv, [30 July 2020] https://doi.org/10.1101/2020.07.29.20161166).

Methods

A detailed methodology can be found in the online supplement. This prospective observational study was conducted at the Royal Women's Hospital in Melbourne, Australia. Ethics approval was granted by the Royal Women's Hospital Human Research and Ethics Committee (#16–33), and the study was registered with the Australian New Zealand Clinical Trials Registry (ACTRN12618000128291).

Infants were eligible for enrollment if they were delivered by elective cesarean section via spinal anesthesia for nonfetal reasons at 36^{+0} or more weeks gestation, and written prospective parental consent obtained. Infants were not included if placement of an EIT belt would interfere with clinical care (24–26) or if the fetus had a known congenital condition that would alter EIT interpretability. Infants who received resuscitative interventions were excluded from analysis.

Measurements

Heart rate and peripheral oxygen saturation (Sp_{O_2}) were measured with a Radical 7 pulse oximeter (Massimo Corporation). Regional lung volume changes were imaged at 48 frames/s with the Pioneer EIT system using an ultrasound gel–coated NeoSensor Belt (Sentec AG) (2, 12, 24–26). Audio and video were recorded at 30 frames/s (webcam; Logitech).

Delivery Room Protocol

As the infant was being placed supine on the resuscitaire, the NeoSensor Belt was secured (velcro tab) around the chest at nipple level (*see* Video E1 in the online supplement). The pulse oximetry sensor was applied to the right hand. There was no other interference with routine clinical care. Infants were managed in a supine position in accordance with local guidelines, including timing of umbilical cord clamping. Data were only recorded during care on the resuscitaire.

Data Acquisition and Analysis

EIT, video, audio, and pulse oximetry data were continuously recorded digitally during resuscitaire management, and timing of critical events from birth were documented. Sp_{O_2} and heart rate data were reviewed for loss of signal or movement artifact. EIT data were recorded in a custom-built infant imaging package (27), and images were reconstructed *post hoc* (19, 28) using the vendor-provided human model chest atlas, with nonlung regions excluded (2, 23, 24, 26). Each potential V_T change due to breathing was identified from the global lung signal. Analysis of the EIT change associated with a breath was only performed if there was *1*) video confirmation

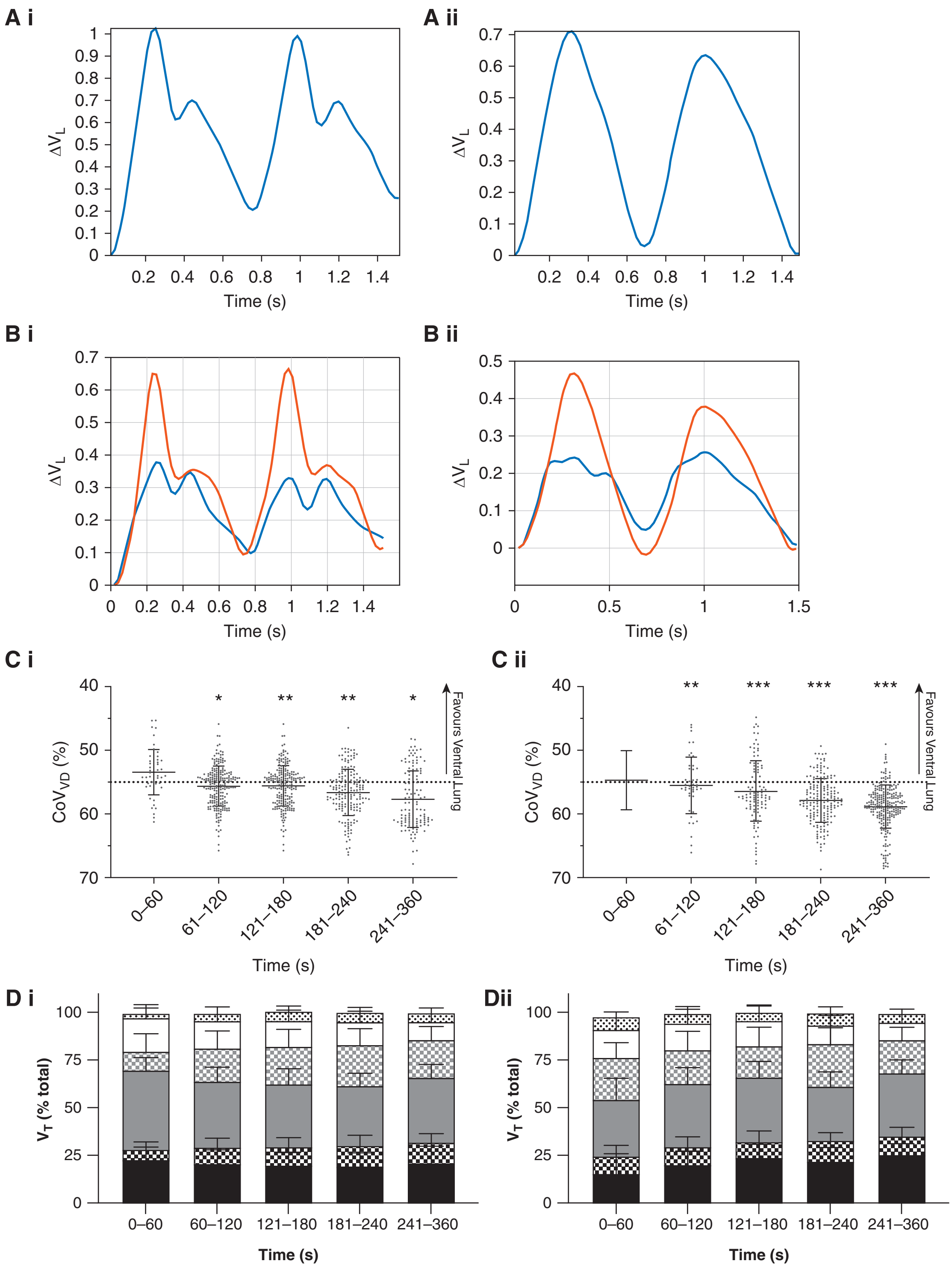

Figure 1. (*A*) Relative volume change (ΔV_L) over time within the whole lung during the two representative breaths for crying (*i*; 25 s) and tidal breaths (*ii*; 5 min). (*B*) ΔV_L during the same breaths within the ventral (blue) and dorsal (red) hemithoraces. (*C*) Ventrodorsal center of ventilation (CoV_{VD}) by minute after birth for crying and tidal breaths. CoV_{VD} of 55% represents uniform ventilation, with values <55% indicating relatively greater ventilation in the ventral lung and >55% indicating greater ventilation in the dorsal lung. Gray dots represent individual breath data, and black lines and bars represent mean ± SD. (*D*) Relative distribution of ventilation (percentage total V_T) along the gravity-dependent plane for crying and tidal breaths in the most gravity-dependent third of the lung (black bars), central third (gray bars), and non–gravity-dependent third (white bars), with solid bars being the right lung region and dotted or checkered bars being the left lung. All data are mean + SD. $^*P < 0.05$, $^{**}P < 0.01$, and $^{***}P < 0.0001$ against first 60 seconds (mixed-effects model).

Table 1. Type of Breath by Time

Included Inflations ($n = 1,401$)	Time from birth					
	0–60 s	61–120 s	121–180 s	181–240 s	241–360 s	Total
Cry, n	55	186	221	188	137	787
Tidal, n	13	48	106	189	258	614
Cry, %*	80.9	79.5	67.6	49.9	34.7	56.2
Cry/infant median (minimum–maximum)	6 (2–21)	13 (3–22)	13 (3–52)	12 (1–63)	15 (1–48)	11 (1–63)
Tidal/infant, median (minimum–maximum)	7 (4–9)	4 (1–13)	9 (1–20)	11 (2–44)	15 (4–102)	9 (1–102)

*$P < 0.0001$; χ^2 test for trend.

of a breath and *2*) no movement interference on the video. All included breaths were classified by the presence of an audible cry, grunt, or no breathing noise (tidal breath). If audio classification was not possible, the breath was excluded (Figure E1).

For included breaths, the prebreath and postbreath FRC, inspiratory time (Ti), expiratory time (Te), time constant of the respiratory cycle (τ), and relative peak inspiratory flow (PIF) and expiratory flow (PEF) were calculated for the global signal and right, left, ventral, and dorsal lung regions (19). The shape of the impedance change during each breath was classified by an investigator (D.G.T.) unaware of the breath type or time from birth. The centers of ventilation along the ventrodorsal (CoV_{VD}) and right–left (CoV_{RL}) planes were calculated to determine spatiotemporal distribution of VT within the chest slice (19, 29). The percentage of the global VT signal was calculated for the most dependent, central, and nondependent thirds of the right and left lung regions, and the percentage and location of lung regions without any VT signal were calculated (19, 24).

Sample Size and Statistical Analysis

Based on a previous study of respiratory parameters at birth (16), a convenience sample of 30 infants was estimated to provide data for breath-by-breath classification and analysis of 100–150 breaths/infant per 5–6-minute period in 15–20 infants. Continuous data were analyzed with a mixed-effects linear regression model, with robust SE and cluster analysis to adjust for multiple breaths from each infant. A *P* value of less than 0.05 was considered statistically significant.

Results

A visual abstract of the main study findings is available in Video E2.

Study Population

Thirty-three families were approached on the day of the delivery, with three declining to participate. Two studied infants received resuscitative support after birth and were excluded. Of the remaining 28 infants, EIT data were obtained in 27 infants (EIT belt incorrectly placed). Complete audio or video data were not acquired in 10 infants (technical failure in delivery room, camera obstructed, excessive background noise, or inability to delineate any audio/video breaths). The characteristics of the final 17 infants with matched EIT, video, and audio data are described in Table E1. All were singleton pregnancies, and no mother received antenatal corticosteroids.

Pulse Oximetry

A pulse oximetry signal could be acquired in 15 infants, with a median (range) of 17 (3–198) seconds between applying the probe and signal acquisition. The first Sp_{O_2} signal was acquired at 52 (12–97) seconds but was then lost for more than 10 seconds at least once in 10 infants. Sp_{O_2} increased with time from 53% (48–72%) at 60 seconds to 78% (60–96%) by 360 seconds ($P = 0.029$; mixed-effects model, Figure E2). Heart rate was stable throughout the study period ($P = 0.25$).

Time to Image Acquisition

The median (range) time from birth to first EIT image was 36 (20–62) seconds, with the longest periods being in the two infants born with delayed cord clamping (60 and 62 s). The time between cutting of umbilical cord and first EIT image was 31 (20–48) seconds. In all infants, the time between applying the EIT belt and first images was less than 12 seconds, with no subsequent signal loss.

Breathing Patterns

A total of 1,401 inflations met the inclusion criteria (Table 1). Only 14 breaths (1%) had audible grunting (all during periods of crying) and were included within the 787 crying breaths. Overall, crying was more prominent early in the respiratory transition, representing 80.9% of all included inflations within the first minute, then decreasing to 34.7% by the sixth minute ($P < 0.0001$; χ^2 test for trend).

Breaths could be classified as following two distinct EIT volume patterns, as follow: *1*) linear inspiratory and expiratory volume change consistent with tidal ventilation of already aerated lungs or *2*) an expiratory phase with a distinct bifid expiratory wave and a transient increase or preservation in lung volume (Figure 1 and Video E2). During these bifid waves, there was a subtle redistribution of ventilation seen on functional EIT images consistent with pendelluft flow. Most (70.8%) crying breaths had a bifid wave, compared with only 2.5% of tidal breaths.

Ti increased over the first minutes of life for both breath types; $P < 0.0001$ (Figure 2A). Crying generated shorter Ti than tidal breaths in the first 60 seconds, with a mean (95% confidence interval [CI]) difference of 101 (56–147) milliseconds. In contrast, Te and τ were longer during crying than tidal breaths (both $P < 0.0001$; Figures 2B and 2C), especially between 61 and 180 seconds (Te) and after 120 seconds (τ). Overall, Te and τ did not change significantly with time for crying or tidal breaths.

PIF was greater at all time epochs during crying compared with tidal breaths (all $P < 0.0001$). Overall, PIF increased with time for tidal breaths ($P < 0.0001$; Figure 2D) but not during crying. PEF was greater during crying than tidal breaths for the first 180 seconds (all $P < 0.0001$; Figure 2E), with the greatest difference in the first 60 seconds (1.4 [0.9–1.8] AU/s). PEF decreased with with time during crying ($P < 0.0001$), whereas tidal breaths were unchanged.

The detailed spatiotemporal behavior of Ti, Te, τ, PIF, and PEF in the right, left, ventral,

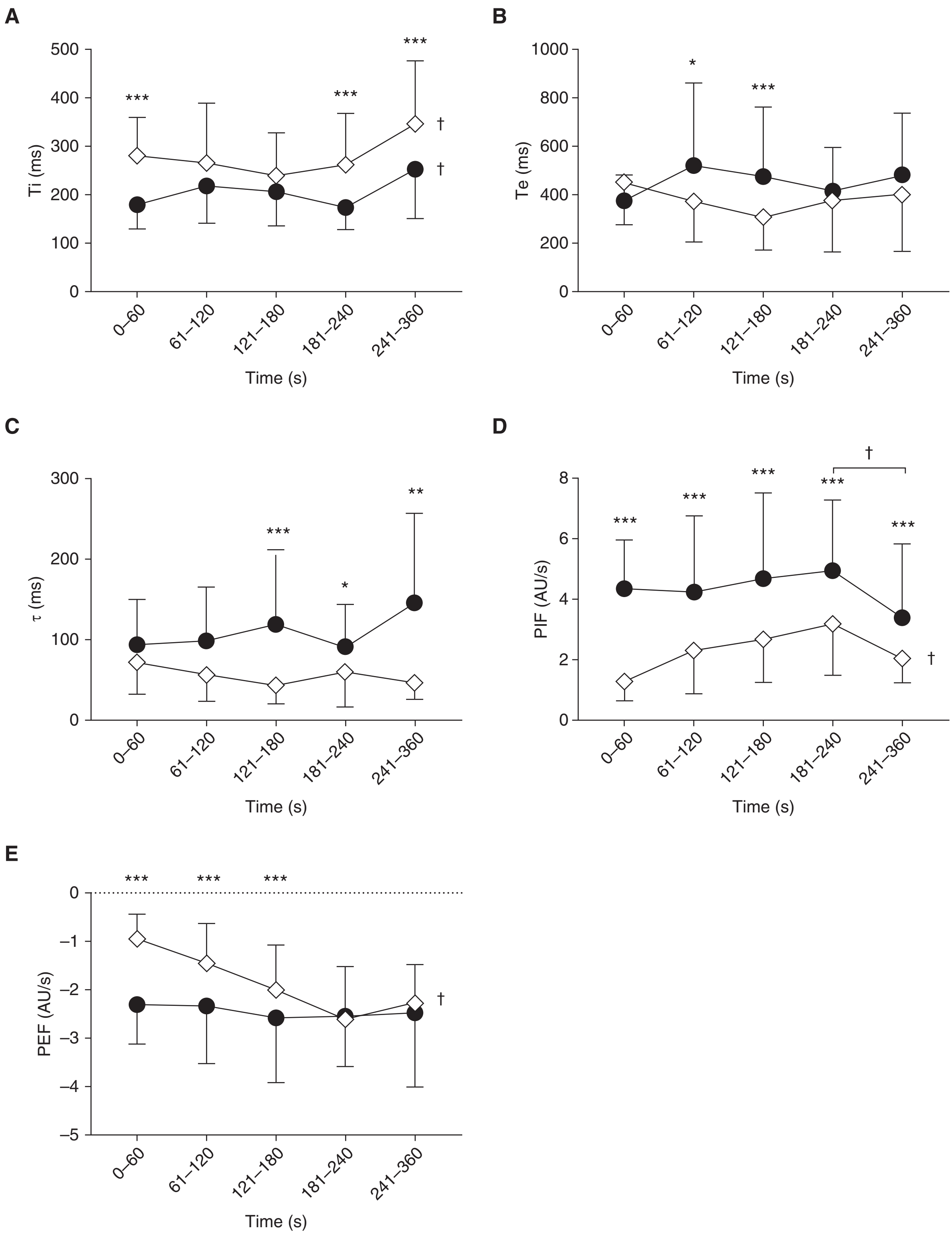

Figure 2. (*A*) Ti, (*B*) Te, (*C*) τ, (*D*) PIF, and (*E*) PEF. Solid circles indicate crying breaths, and open diamonds indicate tidal breaths. All data are mean ± SD. $^{*}P<0.05$, $^{**}P<0.01$, and $^{***}P<0.0001$ cry versus tidal inflation; $^{\dagger}P<0.01$ within breath type (all mixed-effects model). PEF = peak expiratory flow; PIF = peak inspiratory flow; Te = expiratory time; Ti = inspiratory time; τ = respiratory system time constant.

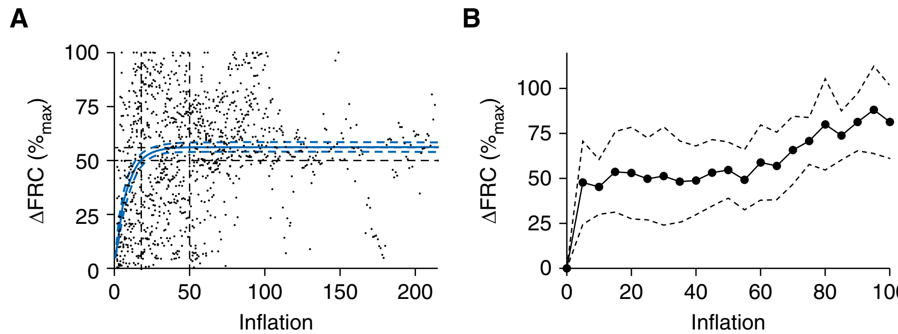

Figure 3. (*A*) Change in FRC (ΔFRC) from first measured inflation for all breaths and (*B*) for the first 100 inflations (maximum). ΔFRC normalized to the FRC before the first breath (0%) and maximum FRC (100%) for each infant. (*A*) Blue line represents the line of best fit (dashed lines represent the 95% confidence interval [CI]) using a one-phase exponential association; $y = y_{plateau}\,[1-e^{x.\tau-1}]$; plateau (95% CI), 56.2% (54.0–58.6%); τ, 8.0 (6.0–10.5) inflations (R^2 0.14; root mean square error 24.5%; replicates test discrepancy, 0.82 [$P = 0.96$]). Gray dashed lines demonstrate ΔFRC at 50% of FRC_{max} and 50 inflations. (*B*) Solid circles represent the mean ΔFRC every five inflations for each infant, and dashed lines represent the 95% CI.

and dorsal regions are provided in the online supplement (Figures E3–E7). Overall, Ti, Te, and τ were similar within all regions for both breath types. Crying resulted in faster PIF and PEF in the dorsal and right regions compared with the ventral and left regions, respectively. Tidal breaths resulted in less right–left and ventral–dorsal heterogeneity in PIF and PEF than crying.

Functional Residual Capacity

Overall, FRC increased and was quickly established after birth, with the maximum recorded FRC value for each infant occurring at a median (interquartile range) of 43 (21–77) of included breaths after birth and in 67.8% (51.9–94.5%) of the analyzed sequential breaths (Figures 3 and E8). During an infant's first 100 breaths (or total if less than 100), 48% of FRC change occurred by the fifth breath.

Regional Ventilation Patterns

Ventilation redistributed toward the dorsal regions with time for both crying and tidal breaths (Figure 1) (CoV_{VD}, $P = 0.045$ and $P < 0.0001$, respectively). Overall, CoV_{VD} favored the ventral regions during crying compared with tidal breaths by a mean (95% CI) of 1.6% (0.3–2.9%), although the differences were not significant within each minute. The redistribution of V_T toward the dorsal regions was predominantly due to increased V_T within central regions during crying and within the dorsal region during tidal breaths ($P = 0.0004$), both at the expense of ventral V_T.

Both breath types resulted in greater ventilation in the right lung (Figure 4). During crying a mean (SD) of 82.2% (15.3%) of total V_T occurring in the right lung during the first 60 seconds (CoV_{RL}, 3.0% [9.1%]; ideal, 46%), increasing within the left lung with time ($P = 0.011$). By 240 seconds, 64.3% (11.4%) of V_T occurred within the right lung (CoV_{RL}, 43.1% [6.5%]). The right lung accounted for the predominance of 59.5% (14.3%) of V_T (CoV_{RL}, 46.4% [9.3%]) during tidal breaths within the first 60 seconds, and this predominance did not change over time ($P = 0.10$). Crying resulted in greater right–left lung inhomogeneity, with CoV_{RL} being a mean (95% CI) of 2.0% (0.5–3.5%) less overall than tidal breaths, and the difference was greatest in the first minute (13.4% [6.7–20.1%]).

Approximately 10% of predefined lung regions were unventilated for both tidal and crying breaths, with no difference in the ventrodorsal pattern of unventilated regions (Figure E9). After 240 seconds, there were fewer unventilated lung regions, especially during tidal breathing, suggesting that increasing aeration resulted in greater engagement of the distal lung in ventilation.

Discussion

The transition to air-breathing at birth is a seminal physiological event essential to life in all humans. In our observational study, we provide the first detailed description of the volumetric processes within the lung at birth. We found that the transition to air-breathing is characterized by complex spatiotemporal patterns of aeration and ventilation initially mediated by high PIF rates and prolonged expiration. Overall, this results in rapid lung aeration that moves from the central to distal lung, with the right lung engaging in ventilation earlier than the left. Crying, the dominant breathing pattern at birth, creates greater PIF and complex expiratory volume patterns, including pendulluft flows, more suited to both rapid aeration and maintenance of FRC than tidal breathing, at a time the lung is still likely to be partially fluid filled. That these findings occurred in healthy term infants without instrumentation or active intervention is important, providing the first human evidence that successful aeration at birth is dependent on actively engaging in expiratory mechanisms to protect FRC (Figure 5).

Clearing the respiratory system of fetal lung liquid and establishing aeration is essential to physiological success at birth. We showed that the majority of lung aeration is rapidly achieved at birth, similar to chest radiography studies during the first seconds after birth in term infants (7, 8). Unlike these studies, we were able to continuously follow the process of aeration beyond the first inflations. Although there was considerable intersubject variability, aeration conformed with an exponential pattern reported in preclinical studies (3, 4, 23, 30, 31) and during lung recruitment in the already aerated lung (32, 33). Aeration was also associated with a temporal increase in distal lung ventilation. Our study is the first in humans to confirm the sequential central–distal movement of the air–fluid interface during aeration from the major airways to the distal alveoli reported in animal studies ongoing beyond the first few breaths (1, 9). EIT cannot directly measure airspace fluid, but the markedly different electrical properties of air and fluid make EIT ideally suited to mapping the air–fluid interface and tracking lung aeration clinically.

The patterns of ventilation indicate that spatiotemporal aeration after birth is more complex than only a central–distal process.

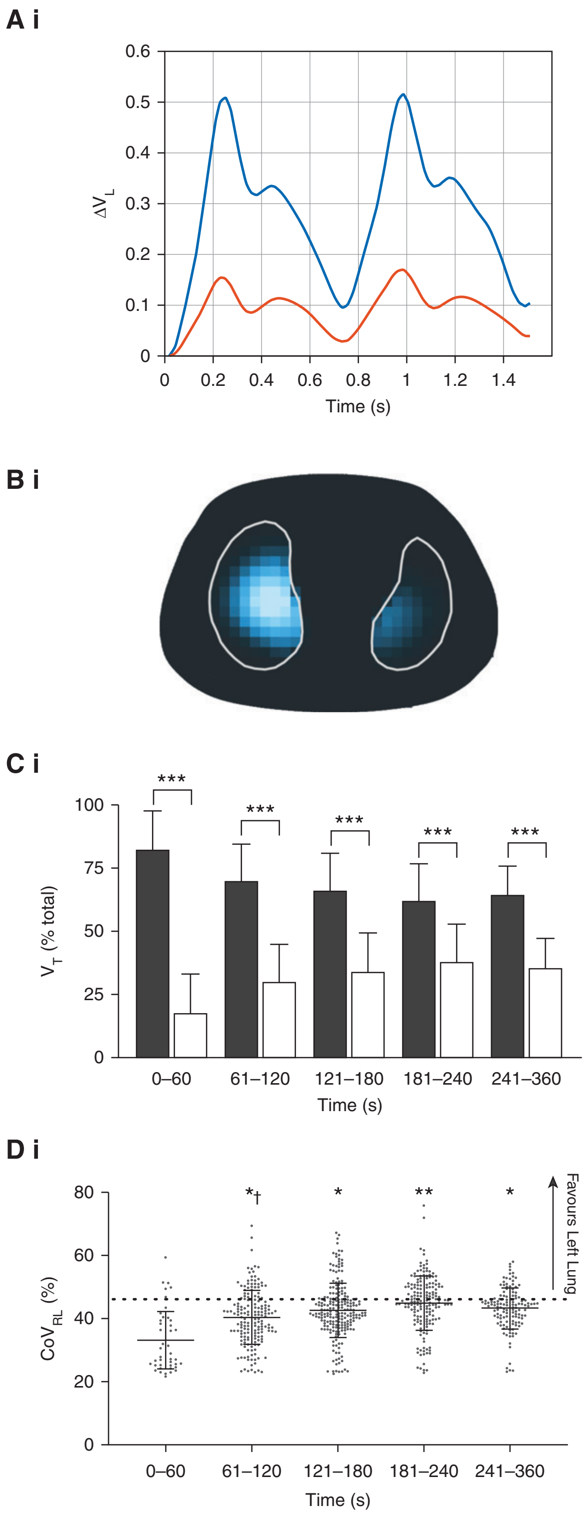

Figure 4. (*A*) ΔV_L over time within the right (blue) and left (red) lung during the two representative breaths for crying (*i*; 25 s) and tidal breaths (*ii*; 5 min). (*B*) Functional electrical impedance tomography images of volume change within the lungs for the same breaths using the color scale defined in Video E2. (*C*) Relative distribution of ventilation (% total V_T) in the right (solid bars) and left (open bars) lung for crying and tidal breaths. (*D*) Center of ventilation along the right–left plane (CoV_{RL}) for all inflations by minute after birth for crying and tidal breaths. CoV_{RL} of 46% represents uniform ventilation, with values <46% indicating relatively greater ventilation in the right lung and values >46% indicating greater ventilation in the left lung. All data are mean ± SD, and dots represent individual breath data. (*A* and *C*) $^*P<0.05$ and $^{***}P<0.0001$ (mixed-effects model). (*B* and *D*) $^*P<0.05$ and $^{**}P<0.01$ against first 60 seconds. $^{\dagger}P<0.05$ against 181–240 seconds. ΔV_L = relative volume change.

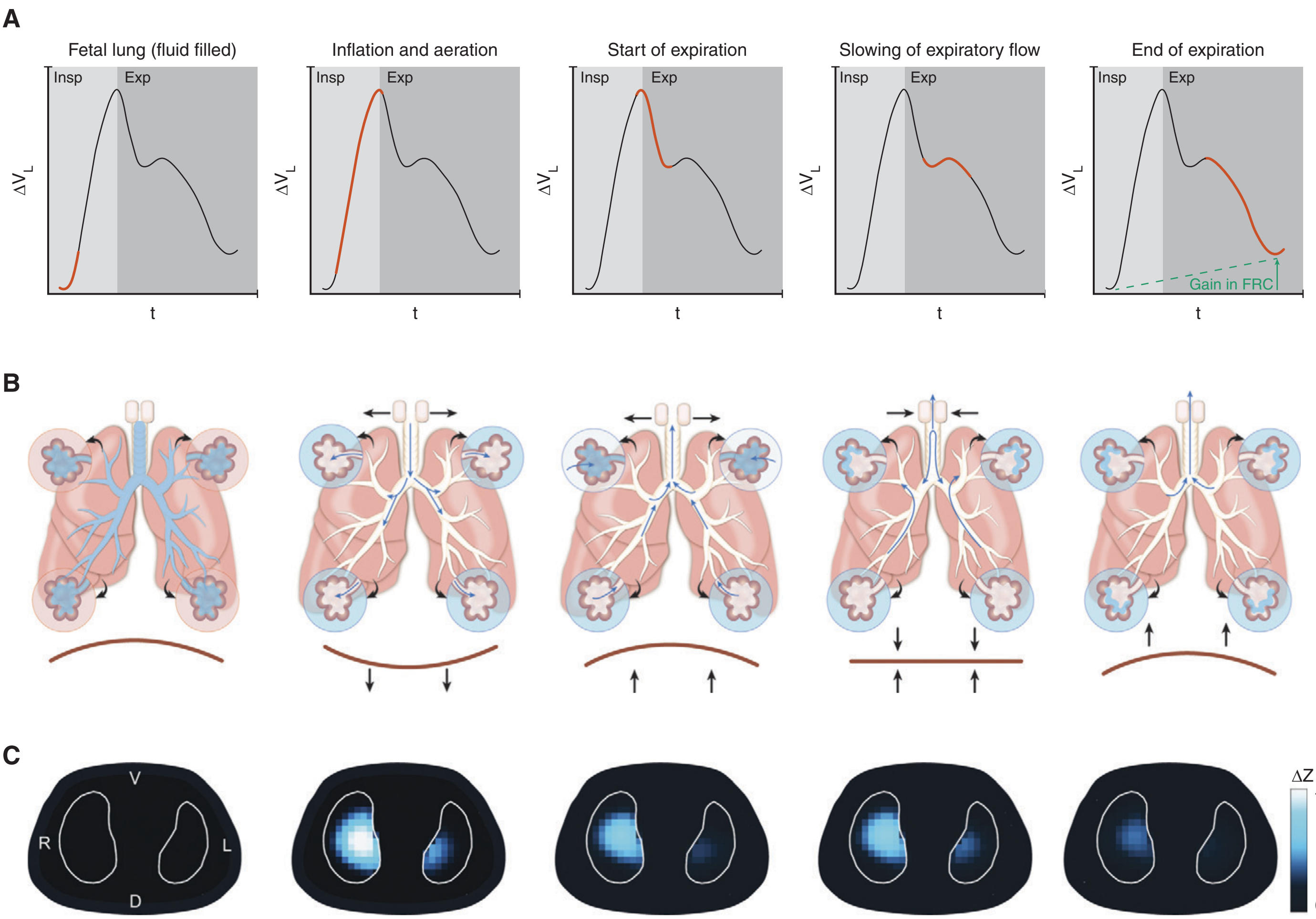

Figure 5. Summary of main findings and hypothesized explanation of the criteria which define the respiratory events within the lungs at birth. Representative global lung volume change during a single cry at 14 seconds after birth (Infant 6; [*A*]) demonstrating the dynamic volume change during inspiration and expiration, and resultant increase in end-expiratory FRC. The breath has been divided into five phases related to the mechanistic events identified during (*B*) the respiratory transition from a fluid-filled to aerated lung, and (*C*) the respective functional electrical impedance tomography images for each. At the start of the inflation, the airways and alveoli are fluid filled (column 1). A cry initiates a rapid and large contraction of the diaphragm with a resultant rapid inspiratory flow (slope of the time–volume curve) and high inflating (driving) pressure within the lung generating aeration by moving fluid from the proximal airways to the alveoli (enlarged) and then the lung interstitium (column 2). Expiration begins with rapid contraction of the diaphragm (column 3). The fall in intrathoracic pressure during expiration lowers intraalveolar pressure, and, in some lung units, this fall allows fetal fluid to influx back into the alveoli spaces. To counteract this effect, the neonate slows (brakes) diaphragmatic contraction and partially closes the glottis, thus transiently repressurizing the lung and allowing pendulluft gas flow between aerated and poorly aerated lung units (column 4). When expiration continues, it does so against a partially closed glottis, which mediates slower expiratory gas flow and allows some gas to remain in the lungs, thus generating a greater end-expiration FRC (column 5) and more favorable lung conditions at the start of the next inflation.

The preferential ventilation of the right lung was unexpected but biologically plausible. At birth, the lung is fluid filled, and airways (and tissue) have a high resistance (34). The left main bronchus exits the carina acutely and is encumbered by the heart. This may create preferential flow states toward the right lung, especially during the higher inspiratory flows of crying. Resistance falls in those areas of the lung that aerate first, further potentiating ventilation compared with unaerated regions. Our data also suggest that ventilation initially follows a gravity-dependent pattern similar to that seen in parenchymal lung diseases (35, 36). Once aerated, the lung rapidly develops the anatomical ventrodorsal pattern of ventilation reported in healthy older infants, favoring the dorsal lung with its increased lung mass and greater diaphragmatic tidal movement (19, 37). These changing spatiotemporal patterns across multiple planes make applying respiratory support without risking lung injury particularly challenging.

As expected in healthy infants, during the first 2 minutes, 80% of breaths were cries. In a similar population of 13 infants, 77% of the analyzed 749 breaths within the first 90 seconds after birth were classified as cries or grunts, but breath classification was performed *post hoc* from face mask measurements without auditory or visual confirmation, limiting interpretability (16). Our study is the first to classify volume changes with flow and breathing behavior. Crying created different flow characteristics than tidal breathing, quickly inflating the lung with faster Ti and PIF. This is advantageous within the highly resistive fluid-filled lung at birth (34), but once the lung is aerated, it provides little mechanical or gas exchange benefit. We postulate that crying has a *de novo* physiological purpose and is not simply due to the noxious stress response of birth. Once aerated, the high PIF conditions of crying increase unventilated lung tissue, with infants switching to the more advantageous tidal breaths.

Importantly, crying is also an expiratory phenomenon, being associated with slow expiratory flows and longer Te and τ. Volume loss during expiration followed a unique bifid pattern, occurring in 71% of all cries and rarely in tidal inflations. This pattern of volume change represents transient periods of minimal airway flow despite the chest wall being in a state of expiratory recoil. In this state, reducing expiratory flow could only be achieved via active means, such as glottic closure or diaphragmatic hold, which are both seen in radiological imaging at birth (8). The lung is in a state of flux in early exutero life; the alveoli maybe air filled but fetal lung fluid remains in the interstitium, and fluid can influx back into alveoli if the intrathoracic pressure gradient falls, compromising FRC (4, 9, 34). It has been proposed that "expiratory braking" is essential during this period (1, 5, 7, 8, 17, 18, 38), and flow patterns measured at the airway opening support this but have not been correlated with temporal FRC change (16). Our study provides the first evidence that expiratory braking does more than just prevent the egress of gas from the lungs. It also facilitates the volumetric conditions needed to preserve FRC and, importantly, redistributes gas within the lungs (pendelluft flow). We propose that this provides a simple visual indicator of an infant's ability to independently support respiratory transition. Further studies are warranted to determine whether the same breath types and patterns are present in at-risk and preterm infants.

Reports of the cardiorespiratory processes at birth are sparse, mainly because of challenges in measurement. After chest radiology studies in the 1960s (7, 8), instrumentation within the mouth, initially with bulky equipment (5, 17, 18, 38) and more recently with face masks (16, 39, 40), have measured airway opening flow, V_T, expired CO_2, and/or pressure changes and infer intrathoracic conditions. Face masks are frequently applied with a leak (41, 42); application interferes with normal breathing efforts (43) and cannot identify important spatiotemporal events, limiting usefulness during spontaneous breathing. Ideally, measurements should be obtained from the thorax without impacting respiratory effort. Recently, respiratory-inductive plethysmography (39) and lung ultrasound (15) have been used in the delivery room. Inductive plethysmography requires two belts and determines lung volume from measuring the cross-sectional areas of the chest and abdomen, which may not change between fluid- and air-filled states (32). Lung ultrasound is ideal for imaging the air–fluid interface and is simple to use but lacks regional resolution, and continuous imaging has not been possible (15). In this context, EIT is attractive. EIT is an established and validated method of measuring relative change in multiple spatiotemporal respiratory parameters (19). EIT is radiation free and available with a simple noninvasive belt (25) that could be applied as quickly, and more reliably, than pulse oximetry. EIT also confirmed the physiological patterns seen in humans and preclinical studies using these other measurement tools (2, 9, 23). We contend that EIT is currently the best method of monitoring the respiratory system at birth.

Limitations

Our study was limited to birth via elective cesarean section, and measurements were not made from delivery of the chest. The birth experience is uniquely personal, and we intentionally limited our study to a period of clinical mother–baby separation. Consequently, we missed the first few inflations in most infants. We contend that these inflations are unlikely to be markedly different from those we captured. The unique volumetric, flow, and FRC characteristics we identified indicate fluid clearance was still ongoing during the first 120 seconds. It is unlikely that the enhanced lung liquid clearance provided by delivery through the vaginal canal would alter the respiratory findings in our healthy term population with active vigorous breathing. Respiratory effort was not suppressed, but data on all modes of delivery are needed in less vigorous infants. We have demonstrated that EIT can be practically applied earlier and during vaginal delivery. Our study of 1,401 inflations from 17 infants is one of the largest, but, like previous studies (16, 17), exclusions were necessary and may have included potentially important breaths. In part, this was intentional; our methodology was designed to minimize artifact and ensure correct breath classification lacking in previous studies (16). It is possible that respiratory drive occurred with an occluded airway. This would not result in a volume change on EIT but is an important physiological finding that should be seen on video. Like all other imaging tools used to describe the respiratory transition, EIT is limited to a single slice of the lung. However, single-slice EIT has been shown to represent whole lung patterns in infants (19). EIT cannot measure intrathoracic pressure. To do so would require invasive instrumentation, but this is unnecessary as flow patterns reflect intrathoracic pressure states.

Conclusions

This study provides the first detailed description of the respiratory behavior of the healthy human lung during the transition to air-breathing after birth. Birth requires rapid aeration of the lung, and this is achieved predominately via crying. Crying creates unique flow and volume states not seen elsewhere in respiratory physiology and is characterized by high PIF and expiratory braking to preserve attained FRC and allow volume redistribution. The right lung ventilates before the left lung after birth, and the lung quickly develops an anatomical pattern of ventrodorsal ventilation once aerated. Understanding how the human lung successfully commences breathing at birth is the first step in developing tools to identify when intervention is required. ■

Author disclosures are available with the text of this article at www.atsjournals.org.

Acknowledgment: The authors thank the families, infants, and Royal Women's Hospital staff involved in the study. The authors also thank Dr. Kate Patterson of Medipics and Prose for assistance with figures and videos and thank Dr. Louise Owen and Dr. C. Omar Kamlin at the Royal Women's Hospital for advice on study implementation in the delivery room.

References

1. Hooper SB, Te Pas AB, Kitchen MJ. Respiratory transition in the newborn: a three-phase process. *Arch Dis Child Fetal Neonatal Ed* 2016;101:F266–F271.
2. Tingay DG, Pereira-Fantini PM, Oakley R, McCall KE, Perkins EJ, Miedema M, *et al.* Gradual aeration at birth is more lung protective than a sustained inflation in preterm lambs. *Am J Respir Crit Care Med* 2019;200:608–616.
3. Tingay DG, Rajapaksa A, Zonneveld CE, Black D, Perkins EJ, Adler A, *et al.* Spatiotemporal aeration and lung injury patterns are influenced by the first inflation strategy at birth. *Am J Respir Cell Mol Biol* 2016;54:263–272.
4. Tingay DG, Lavizzari A, Zonneveld CE, Rajapaksa A, Zannin E, Perkins E, *et al.* An individualized approach to sustained inflation duration at birth improves outcomes in newborn preterm lambs. *Am J Physiol Lung Cell Mol Physiol* 2015;309:L1138–L1149.
5. Milner AD, Vyas H. Lung expansion at birth. *J Pediatr* 1982;101:879–886.
6. van Vonderen JJ, Te Pas AB. The first breaths of life: imaging studies of the human infant during neonatal transition. *Paediatr Respir Rev* 2015;16:143–146.
7. Fawcitt J, Lind J, Wegelius C. The first breath: a preliminary communication describing some methods of investigation of the first breath of a baby and the results obtained from them. *Acta Paediatr Suppl* 1960;49:5–17.
8. Bosma JF, Lind J. Roentgenologic observations of motions of the upper airway associated with establishment of respiration in the newborn infant. *Acta Paediatr Suppl* 1960;49:18–55.
9. Hooper SB, Kitchen MJ, Wallace MJ, Yagi N, Uesugi K, Morgan MJ, *et al.* Imaging lung aeration and lung liquid clearance at birth. *FASEB J* 2007;21:3329–3337.
10. O'Donnell CP, Gibson AT, Davis PG. Pinching, electrocution, ravens' beaks, and positive pressure ventilation: a brief history of neonatal resuscitation. *Arch Dis Child Fetal Neonatal Ed* 2006;91:F369–F373.
11. Perlman JM, Wyllie J, Kattwinkel J, Wyckoff MH, Aziz K, Guinsburg R, *et al.*; Neonatal Resuscitation Chapter Collaborators. Part 7: neonatal resuscitation: 2015 international consensus on cardiopulmonary resuscitation and emergency cardiovascular care science with treatment recommendations. *Circulation* 2015;132(Suppl 1):S204–S241.
12. Tingay DG, Togo A, Pereira-Fantini PM, Miedema M, McCall KE, Perkins EJ, *et al.* Aeration strategy at birth influences the physiological response to surfactant in preterm lambs. *Arch Dis Child Fetal Neonatal Ed* 2019; 104:F587–F593.
13. Manley BJ, Owen LS, Hooper SB, Jacobs SE, Cheong JLY, Doyle LW, *et al.* Towards evidence-based resuscitation of the newborn infant. *Lancet* 2017;389:1639–1648.
14. Karlberg P. The adaptive changes in the immediate postnatal period, with particular reference to respiration. *J Pediatr* 1960;56:585–604.
15. Blank DA, Kamlin COF, Rogerson SR, Fox LM, Lorenz L, Kane SC, *et al.* Lung ultrasound immediately after birth to describe normal neonatal transition: an observational study. *Arch Dis Child Fetal Neonatal Ed* 2018;103:F157–F162.
16. te Pas AB, Wong C, Kamlin CO, Dawson JA, Morley CJ, Davis PG. Breathing patterns in preterm and term infants immediately after birth. *Pediatr Res* 2009;65:352–356.
17. Vyas H, Milner AD, Hopkins IE. Intrathoracic pressure and volume changes during the spontaneous onset of respiration in babies born by cesarean section and by vaginal delivery. *J Pediatr* 1981;99:787–791.
18. Boon AW, Milner AD, Hopkin IE. Physiological responses of the newborn infant to resuscitation. *Arch Dis Child* 1979;54:492–498.
19. Frerichs I, Amato MB, van Kaam AH, Tingay DG, Zhao Z, Grychtol B, *et al.*; TREND study group. Chest electrical impedance tomography examination, data analysis, terminology, clinical use and recommendations: consensus statement of the TRanslational EIT developmeNt stuDy group. *Thorax* 2017;72:83–93.
20. Tingay DG, Rajapaksa A, Zannin E, Pereira-Fantini PM, Dellaca RL, Perkins EJ, *et al.* Effectiveness of individualized lung recruitment strategies at birth: an experimental study in preterm lambs. *Am J Physiol Lung Cell Mol Physiol* 2017;312:L32–L41.
21. Milesi I, Tingay DG, Lavizzari A, Bianco F, Zannin E, Tagliabue P, *et al.* Supraglottic atomization of surfactant in spontaneously breathing lambs receiving continuous positive airway pressure. *Pediatr Crit Care Med* 2017;18:e428–e434.
22. McCall KE, Waldmann AD, Pereira-Fantini P, Oakley R, Miedema M, Perkins EJ, *et al.* Time to lung aeration during a sustained inflation at birth is influenced by gestation in lambs. *Pediatr Res* 2017;82:712–720.
23. Tingay DG, Bhatia R, Schmölzer GM, Wallace MJ, Zahra VA, Davis PG. Effect of sustained inflation vs. stepwise PEEP strategy at birth on gas exchange and lung mechanics in preterm lambs. *Pediatr Res* 2014;75:288–294.
24. Tingay DG, Waldmann AD, Frerichs I, Ranganathan S, Adler A. Electrical impedance tomography can identify ventilation and perfusion defects: a neonatal case. *Am J Respir Crit Care Med* 2019;199:384–386.
25. Sophocleous L, Frerichs I, Miedema M, Kallio M, Papadouri T, Karaoli C, *et al.* Clinical performance of a novel textile interface for neonatal chest electrical impedance tomography. *Physiol Meas* 2018;39:044004.
26. Miedema M, Waldmann A, McCall KE, Böhm SH, van Kaam AH, Tingay DG. Individualized multiplanar electrical impedance tomography in infants to optimize lung monitoring. *Am J Respir Crit Care Med* 2017;195: 536–538.
27. Adler A, Lionheart WR. Uses and abuses of EIDORS: an extensible software base for EIT. *Physiol Meas* 2006;27:S25–S42.
28. Adler A, Arnold JH, Bayford R, Borsic A, Brown B, Dixon P, *et al.* GREIT: a unified approach to 2D linear EIT reconstruction of lung images. *Physiol Meas* 2009;30:S35–S55.
29. Frerichs I, Becher T. Chest electrical impedance tomography measures in neonatology and paediatrics-a survey on clinical usefulness. *Physiol Meas* 2019;40:054001.
30. Siew ML, Te Pas AB, Wallace MJ, Kitchen MJ, Lewis RA, Fouras A, *et al.* Positive end-expiratory pressure enhances development of a functional residual capacity in preterm rabbits ventilated from birth. *J Appl Physiol (1985)* 2009;106:1487–1493.
31. te Pas AB, Siew M, Wallace MJ, Kitchen MJ, Fouras A, Lewis RA, *et al.* Establishing functional residual capacity at birth: the effect of sustained inflation and positive end-expiratory pressure in a preterm rabbit model. *Pediatr Res* 2009;65:537–541.
32. Tingay DG, Mills JF, Morley CJ, Pellicano A, Dargaville PA. The deflation limb of the pressure-volume relationship in infants during high-frequency ventilation. *Am J Respir Crit Care Med* 2006;173:414–420.
33. Miedema M, de Jongh FH, Frerichs I, van Veenendaal MB, van Kaam AH. Regional respiratory time constants during lung recruitment in high-frequency oscillatory ventilated preterm infants. *Intensive Care Med* 2012;38:294–299.
34. Veneroni C, Tingay DG, McCall KE, Pereira-Fantini PM, Perkins EJ, Dargaville PA, *et al.* Respiratory mechanics during initial lung aeration at birth in the preterm lamb. *Am J Physiol Lung Cell Mol Physiol* 2020;318: L525–L532.
35. Miedema M, de Jongh FH, Frerichs I, van Veenendaal MB, van Kaam AH. Changes in lung volume and ventilation during lung recruitment in high-frequency ventilated preterm infants with respiratory distress syndrome. *J Pediatr* 2011;159:199–205.e2.
36. Gattinoni L, Caironi P, Pelosi P, Goodman LR. What has computed tomography taught us about the acute respiratory distress syndrome? *Am J Respir Crit Care Med* 2001;164:1701–1711.
37. Pham TM, Yuill M, Dakin C, Schibler A. Regional ventilation distribution in the first 6 months of life. *Eur Respir J* 2011;37:919–924.
38. Boon AW, Milner AD, Hopkin IE. Lung expansion, tidal exchange, and formation of the functional residual capacity during resuscitation of asphyxiated neonates. *J Pediatr* 1979;95:1031–1036.
39. van Vonderen JJ, Lista G, Cavigioli F, Hooper SB, te Pas AB. Effectivity of ventilation by measuring expired CO2 and RIP during stabilisation of preterm infants at birth. *Arch Dis Child Fetal Neonatal Ed* 2015;100: F514–F518.
40. Hooper SB, Fouras A, Siew ML, Wallace MJ, Kitchen MJ, te Pas AB, *et al.* Expired CO2 levels indicate degree of lung aeration at birth. *PLoS One* 2013;8:e70895.
41. Schmölzer GM, Dawson JA, Kamlin CO, O'Donnell CP, Morley CJ, Davis PG. Airway obstruction and gas leak during mask ventilation of preterm infants in the delivery room. *Arch Dis Child Fetal Neonatal Ed* 2011;96: F254–F257.
42. Schmölzer GM, Kamlin OC, O'Donnell CP, Dawson JA, Morley CJ, Davis PG. Assessment of tidal volume and gas leak during mask ventilation of preterm infants in the delivery room. *Arch Dis Child Fetal Neonatal Ed* 2010;95:F393–F397.
43. Kuypers KLAM, Lamberska T, Martherus T, Dekker J, Böhringer S, Hooper SB, *et al.* The effect of a face mask for respiratory support on breathing in preterm infants at birth. *Resuscitation* 2019;144:178–184.